

Molecular Alignment and Electronic Structure of *N,N'*-Dibutyl-3,4,9,10-perylene-tetracarboxylic-diimide Molecules on MoS₂ Surfaces

Arramel,^{*,†} Xinmao Yin,^{†,‡,§} Qixing Wang,[†] Yu J. Zheng,[†] Zhibo Song,[†] Mohammad H. bin Hassan,[†] Dianyu Qi,[†] Jishan Wu,^Δ Andriwo Rusydi,^{†,‡,⊥} and Andrew T. S. Wee^{*,†}

[†]Department of Physics, National University of Singapore, 2 Science Drive 3, 117542 Singapore

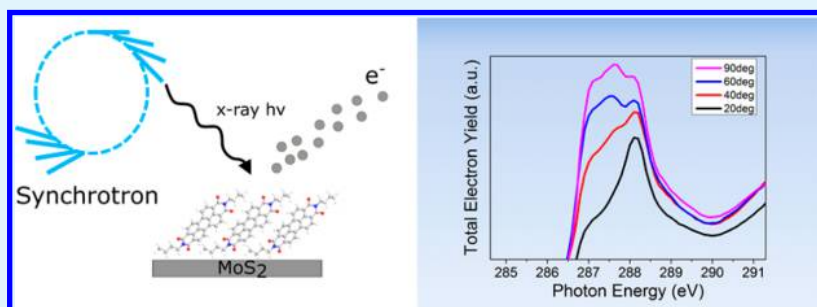
[‡]Singapore Synchrotron Light Source, National University of Singapore, 5 Research Link, Singapore 1176033

[§]SZU-NUS Collaborative Innovation Center for Optoelectronic Science and Technology, Key Laboratory of Optoelectronic Devices and Systems of Ministry of Education and Guangdong Province, Shenzhen University, Shenzhen 518060, China

^ΔDepartment of Chemistry, National University of Singapore, 3 Science Drive 3, 117543 Singapore

[⊥]NUSNNI-NanoCore, National University of Singapore, Singapore 117411

Supporting Information



ABSTRACT: The molecular orientation of organic semiconductors on a solid surface could be an indispensable factor to determine the electrical performance of organic-based devices. Despite its fundamental prominence, a clear description of the emergent two-dimensional layered material–organic interface is not fully understood yet. In this study, we reveal the molecular alignment and electronic structure of thermally deposited *N,N'*-dibutyl-3,4,9,10-perylene-dicarboximide (PTCDI-C4) molecules on natural molybdenum disulfide (MoS₂) using near-edge X-ray absorption fine structure spectroscopy (NEXAFS). The average tilt angle determination reveals that the anisotropy in the π^* symmetry transition of the carbon *K*-edge (284–288 eV range) is present at the sub-monolayer regime. Supported by ultraviolet photoelectron spectroscopy (UPS), X-ray photoelectron spectroscopy (XPS), and resonant photoemission spectroscopy (RPES) measurements, we find that our spectroscopic measurements indicate a weak charge transfer established at the PTCDI-C4/MoS₂ interface. Sterical hindrance due to the C4 alkyl chain caused tilting of the molecular plane at the initial thin film deposition. Our result shows a tunable interfacial alignment of organic molecules on transition metal dichalcogenide surfaces effectively enhancing the electronic properties of hybrid organic–inorganic heterostructure devices.

KEYWORDS: perylene, near-edge X-ray absorption spectroscopy, XPS, UPS, RPES, interface

INTRODUCTION

The electronic structure of two-dimensional layered material such as transition metal dichalcogenides (TMDCs) plays an important role in determining its optical and electrical performance. It can be modified through adsorption of organic compounds on their surfaces that offer a broad range of applications from optoelectronics to gas sensing.^{1–4} To achieve a convenient control of the optical and electrical properties of TMDCs, recent attempts have attempted to chemically dope the TMDCs using gas,⁵ metallic nanoparticle,⁶ or large organic molecules.⁷ Thus, a controllable functionalization of these peculiar layered materials by means of molecular dopants could

be a key step to unlock their potential via surface and interface chemistry.

A few studies have demonstrated that a small contribution of the dispersion force is attributed to the presence of alkyl chains in organic molecular semiconductors.^{8,9} However, the interaction between perylene-based semiconductors and TMDCs is largely unexplored. It is of utmost importance to understand the physical origin and electronic structure behind the energy-

Received: November 1, 2016

Accepted: January 18, 2017

Published: January 18, 2017

level alignment near the Fermi energy, E_F , at hybrid organic/transition metal dichalcogenides interfaces^{10,11} for organic-TMDCs device performance using organic–inorganic hetero-interfaces.¹²

The perylene derivative family is one of the most extensively studied organic semiconductor molecules.^{13–17} In the field of organic electronics, perylene-based molecules are considered good candidates for optoelectronic and photovoltaic device applications due to their ability to form well-ordered assemblies on many surfaces.^{9,18–22} In the previous work of Kampen et al.,²³ the orientation of PTCDI molecules was found to be tilted by about 50° with respect to the GaAs surface. Hiroshiba and co-workers²⁴ evaluated perylene molecules with long alkyl chains (PTCDI-C8) and observed a preferential flat-lying configuration when thermally deposited on a SiO₂/Si surface using X-ray reflection (XRR) measurements. This leads to the question of how the alkyl functional group influences the surface molecular orientation on solid surfaces.

It is of fundamental interest that the RPES measurements of organic molecules on surfaces provide relevant access to gain better physical insight into the charge-transfer dynamics phenomena on surfaces. For instance, Jong et al.²⁵ initiated the implementation of the RPES technique on the femtosecond charge transfer dynamics study of Fe(II)-tetraphenylporphyrin molecules on MoS₂. In addition, our predecessors have contributed to the field by exploring the peculiar finding in the adsorption of the homologue perylene molecule 3,4,9,10-perylene-tetracarboxylic-dianhydride (PTCDA) on the respective Au(111)²⁶ and TiO₂(110)²⁷ substrates. In the latter case, it is of importance to realize that even in such a considered planar molecule, it turns out that the evolution of RPES spectra as a function of PTCDA coverage exhibited a different electronic coupling that originates from a chemical coupling between the substrate and the PTCDA molecules. Therefore, it is appealing that the current interest to investigate the homologue perylene molecules (PTCDI-C4) seems largely unexplored.

In the past decade, recent studies have mainly concentrated on understanding the relationship of the molecular orientation of the organic molecule on the device performance.^{28,29} A detailed understanding of the charge-transfer event of π -conjugated organic semiconductors on a solid surface could become a limiting factor to achieve a highly efficient electrical performance of an organic-based device. In particular, the proper control of molecular arrangement on the semi-conducting substrate can be tailored by manipulating predetermined molecular alignment in the edge-on (orthogonal) or face-on (parallel) configuration. An intriguing question may arise as to whether the outcome of the organic-based device performance is significantly affected if, hypothetically, the oriented molecules could lie between these two well-defined configurations.

In this work, PTCDI-C4 molecules were evaporated on top of freshly mechanically exfoliated natural molybdenum disulfide (MoS₂) to investigate the molecular orientation and energy level alignment at the hybrid organic/inorganic interface. Transition metal dichalcogenides are materials of current interest, especially in 2D van der Waal heterostructures, due to their band gap tunable properties.^{30–34} In addition, this material is chosen owing to its relatively low cost, high earth abundance in natural or geological form, and good optoelectronic response.^{35,36} The physical interaction between organic molecules and the outer layer of MoS₂ consisting of a sulfur–molybdenum–sulfur atom layered structure is scientifically

interesting and potentially useful for device applications involving similar 2D materials. We thermally deposited PTCDI-C4 molecules on MoS₂ by varying the deposition times to form different molecular coverages from a few layers to multilayer thick films. The molecular orientation study of PTCDI-C4 molecules on the MoS₂ substrate is determined by performing angular-dependent NEXAFS measurements. To understand the charge transfer dynamics, the RPES acquisition data were systematically performed on three respective samples. As a result, a weak resonant enhancement of the photoemission signals close the *K*-edge absorption edge is present at the initial formation of PTCDI-C4 thin films on MoS₂. This finding brings us one step closer to understanding the role of molecular orientation to promote an efficient charge-transfer event on emergent two-dimensional layered materials such as the MoS₂ surface.

EXPERIMENTAL SECTION

Sample Preparation. The natural MoS₂ used here was purchased from HQ graphene.³⁷ The samples were mechanically exfoliated to obtain a freshly cleaved surface. The sample was immediately outgassed in a deposition chamber overnight prior to the molecular deposition procedure. PTCDI-C4 molecules were thoroughly degassed for several hours prior to the thermal sublimation procedure using a deposition temperature of 235 °C with growth times of 40 s, 1 min, 3 min, and 5 min, respectively.

NEXAFS Measurements. C *K*-edge NEXAFS experiments were performed at the Surface, Interface, and Nanosstructure Science (SINS) beamline of Singapore Synchrotron Light Source (SSLS) equipped with a Scienta R4000 electron energy analyzer.³⁸ The samples discussed here were deposited in a separate preparation chamber and transferred ex situ to the SINS beamline. Prior to the synchrotron measurements, all of the samples were annealed to minimize adsorbed contaminants. All spectroscopic measurements were performed in an ultrahigh vacuum (UHV) chamber with a base pressure of 1×10^{-10} mbar. The incident photon energy was calibrated using a sputter-cleaned gold foil in electrical contact with the sample. The energy spectra were referenced to the Au 4f_{7/2} core level peak at 84.0 eV. The C *K*-edge NEXAFS spectra were measured in total electron yield (TEY) mode by collecting the sample current with a photon energy resolution of 200 meV. The linear polarization factor of the X-ray beam was determined to be >90%.

AFM Inspection. The morphology of thermally deposited PTCDI-C4 molecules was characterized using a commercial atomic force microscopy (AFM, BRUKER Dimension FastScan) (see the Supporting Information, Figure S1). A standard cantilever with a spring constant of 40 N/m and a tip curvature <10 nm was used as a probe.

XPS and UPS Measurements. XPS measurements were carried out within the same SINS facility with the error limit for the XPS instrument of 0.1 eV. All photoemission spectra were collected at normal emission. The least-squares peak fit analysis was performed using Voigt photoemission profiles to deconvolute the spectra. The UPS experiments were carried out to measure the work function using 60 eV as the photon energy with a –7 V bias was applied to the sample to overcome the work function of the analyzer.

RPES Measurements. RPES spectra were collected at the valence band region with photon energy swept from 280 to 290.3 eV across the C 1s $\rightarrow \pi^*$ resonances. Thus, the spectra were plotted on a binding energy scale with respect to the substrate Fermi level (E_F). The presented spectra have been normalized using the incident photon intensity.

RESULTS AND DISCUSSION

We first oriented the incoming photon beam at low grazing angle (20°) with respect to the sample surface to obtain angular-dependent NEXAFS spectra. In this case the photon

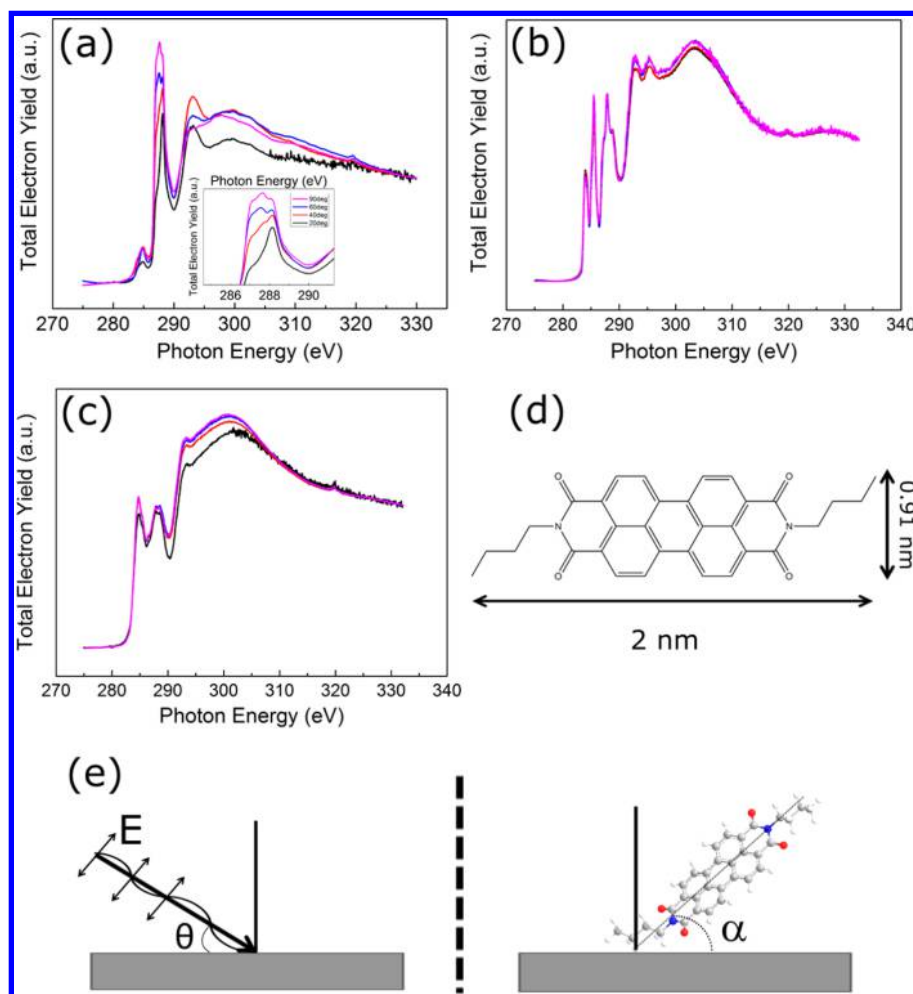


Figure 1. Carbon *K*-edge NEXAFS spectra of PTCDI-C4 film as a function of molecular thicknesses. Spectra were taken at (a) 1 min, (b) 3 min, and (c) 5 min of deposition time. The inset in panel a displays the enlargement of the photon energy range spectra of the respective deposition time centered at 286–290 eV. This energy range is associated with the participating π^* transition symmetry analysis. The angular dependent measurements were taken with 20° (black line), 40° (red line), 60° (blue line), and 90° (pink line) incidence angles. (d) Chemical structure of PTCDI-C4 molecule with the estimated dimensions from the gas phase structure calculation. (e) The left side is a schematic illustration of the NEXAFS geometry used in this study, where θ is the incidence angle. The right side illustrates the molecular conformation with respect to the MoS₂ substrate. α is the average tilt angle.

polarization (E) is mostly out-of-plane with respect to the sample surface. Panels a, b, and c of Figure 1 show carbon *K*-edge NEXAFS spectra at different photon incidence angles of the PTCDI-C4 film as a function of molecular thicknesses with 1, 3, and 5 min deposition times, respectively. The chemical structure of the PTCDI-C4 molecule is presented in Figure 1d. The experimental geometry and the molecular conformation are schematically depicted in Figure 1e. To acquire the angle-dependent measurements, we change the incoming photon beam from 20°, 40°, and 60° to normal incidence (90°).

The NEXAFS spectra at different molecular coverages exhibit distinct peak enhancements due to respective transition resonance states. It is well understood that the resonant intensity is strongly sensitive to the E vector. The intensity is enhanced when E is parallel to the molecular orbital vector. Conversely, the intensity is suppressed when E is perpendicular to the molecular orbital vector.^{39,40} In this analysis, we assign the peaks in accordance to the two regimes (π^* and σ^* electronic transitions) that are commonly found in the 283–290 eV energy range.

The origin of the resonance peak in the NEXAFS spectrum below 285.4 eV corresponds to the π^* resonances due to the electronic transitions from the initial states into the unoccupied π^* molecular orbitals (LUMOs), whereas the 292.4 eV feature is attributed to the σ^* resonances transition into LUMOs. The respective resonance peaks are given in Table 1.

We first discuss the data for the PTCDI-C4 molecule with 1 min deposition time on HOPG (the NEXAFS spectra can be found in the Supporting Information, Figure S2). The assignments of the resonance states are referenced to published

Table 1. Resonance Transition Peaks of PTCDI-C4 Molecules on Different Substrates with Different Deposition Times^a

sample	π_1^* (eV)	π_2^* (eV)	π_3^* (eV)	σ_1^* (eV)	σ_2^* (eV)
1 min on HOPG	282.8	285.3	287.7	292.6	295.3
1 min on MoS ₂	284.9	287.9	288.1	293.4	299.9
3 min on MoS ₂	284.1	285.5	287.9	292.8	295.8
5 min on MoS ₂	284.9	287.9	288.5	293.2	301.2

^aUncertainty in binding energy values is ± 0.05 eV.

literature.^{41–43} We note that the resonance peak positions are consistent with the aforementioned literature. We did not observe any significant angular dependence variation when comparing the π^* perylene core versus σ^* core intensities at different angles of incidence. Thus, we deduce that the PTCDI-C4 molecular orientation is most likely disordered.

In contrast, we find that there is pronounced angular polarization dependence in the NEXAFS spectra of PTCDI-C4 molecules deposited for 1 min on the MoS₂ substrate as depicted in Figure 1a and its enlargement in the inset. The π^* perylene core resonance states are merged into one peak at 284.9 eV for all incidence angle data. On the other hand, the π^* imide group shows a peak centered at 288.0 eV at 20° incidence angle. Surprisingly, the second π^* imide group peak arises at 287.5 and 287.6 eV for 60° and 90° incidence angles, respectively. These observations are somewhat different from the sharp π^* resonant peaks in the PTCDI case.^{42,43} We attribute this difference to the repulsive force caused by sterical hindrance of butyl chains on the MoS₂ surface. The σ^* transition shows a similar broad resonance feature compared to previous findings⁴² in which the maximum intensity at 292.6 eV was reported.

The two NEXAFS spectra displayed in panels b and c of Figure 1 do not show significant angular dependence as compared to Figure 1a. In a multilayer case, intermolecular interactions dominate and molecule–substrate interactions are no longer significant.^{35,36} Consequently, the molecules in the thick films are highly orientationally disordered. To extract the average tilt angle of the molecular plane at different PTCDI-C4 coverages, we assume random azimuthal orientation between the molecule plane and the MoS₂ substrate.^{39,40} The angular-dependent π^* resonance intensity at different incidence angles can be formulated as⁴⁴

$$I\alpha A \times \left\{ \frac{P}{3} \left[1 + \frac{1}{2} (3 \cos^2 \Theta - 1)(3 \cos^2 \alpha - 1) \right] + \frac{(1-P)}{2} \sin^2 \alpha \right\} \quad (1)$$

where A is a constant, $P = 0.90$ corresponds to the linear polarization factor,^{38,45} and α is the average tilt angle of molecular backbone normal to the substrate surface. Linear plots of I versus $\cos^2 \Theta$ were used to extract the slope and intercept, used to determine the unknown parameter, and the average tilt angle (α). From this analysis, we determined the average tilt angles to be $62.3 \pm 0.1^\circ$, $55.0 \pm 0.9^\circ$, and $55.8 \pm 0.3^\circ$ for 1, 3, and 5 min deposition times, respectively (further details can be found in the Supporting Information). For the 1 min sample, we can deduce that the molecule has a stronger tendency to stand upright with respect to the MoS₂ surface. The extracted tilt angles for the other two thicker samples are close to the magic angle (54.7°),⁴⁴ implying that a random PTCDI-C4 molecular orientation exists in the multilayer samples.

Cao et al. demonstrated that the intensity variation of the π^* perylene core peaks was also observed in the case of PTCDA molecular deposition on TiO₂ (110).^{27,45} They deduced that the electronic coupling is largely enhanced by the conformation of the PTCDA molecule at different rutile adsorption sites and that the average tilt angle of PTCDA is influenced by their interaction with the underlying substrate. Cho et al. found that the tilt angle of the PTCDA molecule can be as low as 25° on ITO. However, the molecular tilt angle is increased to 40° when the PTCDA molecule is adsorbed on rutile. There are several studies of PTCDI–substrate interactions that also

indicate that the substrate significantly influences the molecular orientation, and the data are summarized in Table 2. For

Table 2. Comparative Molecular Orientation of Perylene Molecules on Different Substrates^a

molecule on surface	authors	molecular orientation (deg)
PTCDA on ITO	Cho et al. ⁵⁰	25
PTCDA on Au(111)	Cao et al. ⁵¹	27
PTCDA on TiO ₂ (110)	Cao et al. ⁴⁵	40
PTCDI on TiO ₂ (110)	Lanzilotto et al. ⁴²	35
PTCDI-C1 on GaAs (110)	Kampen et al. ²³	50
PTCDI-C4 on alkali halide (001)	Schlettwein et al. ⁴⁶	0
PTCDI-C4F7 on SiO ₂	Schimdt et al. ³⁴	47
PTCDI-C5 on Al ₂ O ₃	Chesterfield et al. ⁴⁷	90
PTCDI-C8 on SiO ₂	Malenfant et al. ⁴⁸	90
PTCDI-C13 on poly(α -methylstyrene)	Rolin et al. ⁴⁹	90
PTCDI-C4 on MoS ₂ (this work)	Arramel et al.	62.3

^aMolecular orientation angle is with respect to the surface.

example, Schlettwein et al.⁴⁶ found that bulk PTCDI-C4 tends to be flat on an alkyl halide (001) surface. In contrast, the longer alkyl substituent perylene derivatives (PTCDI-C5,⁴⁷ PTCDI-C8,⁴⁸ PTCDI-C13⁴⁹) exhibit an upright molecular configuration. Further theoretical simulation studies are recommended to better understand the tilt angle of PTCDI-C4/MoS₂ found in this study.

In our case, we believe that three factors could influence the molecular orientation of PTCDI-C4 molecules on a solid surface: the attractive van der Waals dispersion force due to neighboring alkyl-chain interactions that plays a role in the initial molecular deposition, the π – π stacking of the intermolecular perylene core, and the molecule–substrate interaction strength at the interface. The latter interaction will be discussed in the following section.

To study the interfacial interaction between PTCDI-C4 and MoS₂, X-ray and ultraviolet photoelectron spectroscopies were performed. The evolution of the C 1s core level state of the molecule upon molecular deposition was monitored using XPS in Figure 2a. The main prominent C 1s core level peak is shifted from 283.9 eV (1 min) toward a higher binding energy of 284.1 eV (3 min). Consequently, a chemical shift (~ 0.2 eV) toward higher binding energy was clearly observed as the molecular thickness progressed from a few layers toward thick films (see further detail of peak fitting results in the Supporting Information, Figure S7). In comparison, O'Shea et al.²¹ found a chemical shift of 0.6 eV to lower binding energy of the imide carbon atoms for XPS studies of PTCDI molecules on Au(111) from submonolayer to multilayer thick film. In this case, a non-negligible interaction might occur between the imide ends of the molecule with the underlying gold substrate at the initial first adsorbed molecular layer. Another aspect is found by Addou et al.,³⁶ who proposed surface defects in natural MoS₂ can influence the electronic properties of as-exfoliated MoS₂. According to their findings, the native surface sulfur vacancies led to additional electronic gap states. On the basis of this information, we could infer that gap states due to sulfur vacancies could strongly interact with the PTCDI-C4 molecules via dispersive forces of the butyl chains, consequently mediating the weak interaction between the molecule and the MoS₂

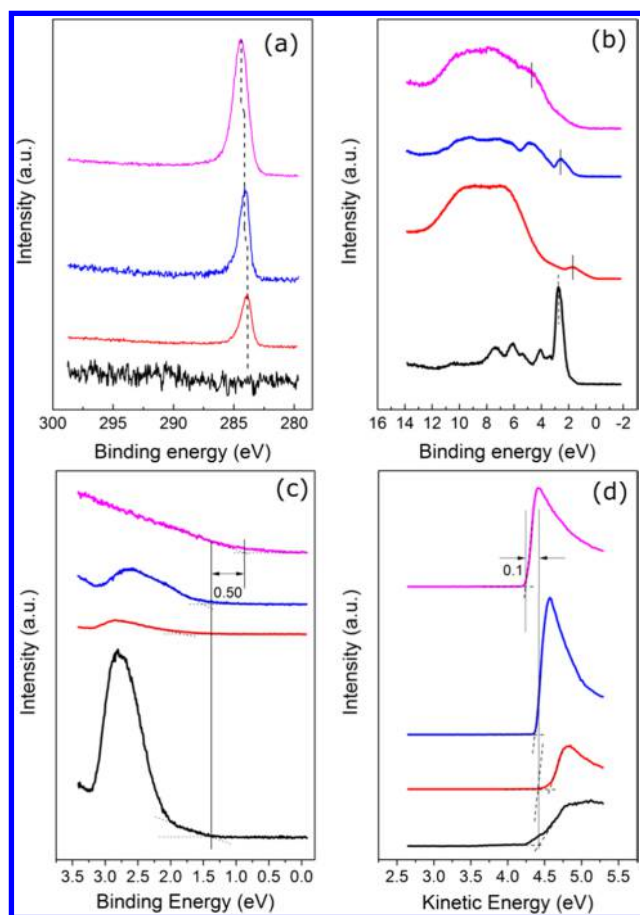


Figure 2. (a) XPS C 1s core level spectra for different molecular coverages. The dashed line serves as a guide to show the chemical shift in these samples. (b) Valence band spectra acquired at different deposition times. Solid line represents the HOMO level progression toward higher binding energy from a few layers to multithick films. (c) Valence bands structure of PTCDI-C4 close to the Fermi level. (d) Work function variation extracted from the secondary cutoff measurements: bare MoS₂ (black); 1 min (red), 3 min (blue), and 5 min (pink) deposition times of PTCDI-C4 molecules.

substrate. Recent studies have shown that the native defect of MoS₂ can influence the device performance and interface electronic properties.^{52–55} Further in situ investigations will be needed to elucidate the exact nature of defects at the PTCDI-C4/MoS₂ interface.

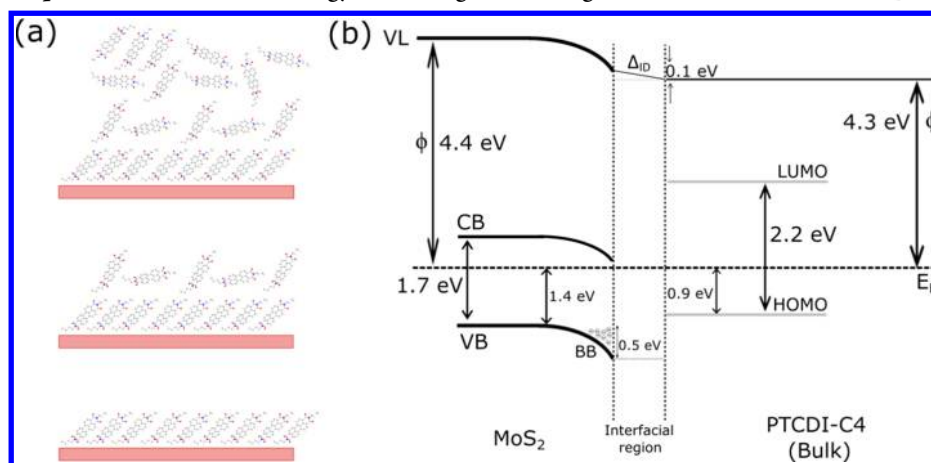
Upon PTCDI-C4 deposition, the highest occupied molecular orbital (HOMO) molecular level emerged and dominated the valence band spectra shown in Figure 2b. This broad feature is completely different from the observed sharp peak close to the E_F (dashed vertical line) of the bare valence band spectrum of MoS₂. The HOMO of a few layers (1 min) PTCDI-C4 on MoS₂ exhibited an asymmetric peak shape at the binding energy of 1.7 eV. The HOMO position is shifted toward higher binding energy (2.6 eV for 3 min and 4.7 eV for 5 min sample) as indicated by the black solid line. To provide more insight into the PTCDI-C4/MoS₂ interface, we discuss the relevant features close to the Fermi energy shown in Figure 2c.

The interpolation of the respective spectrum from the few layer to the multilayer case led to the onset difference of about 0.5 eV. Thus, we can use this value for plotting the energy level alignment in the following passage.

We also explore the evolution of work function upon PTCDI-C4 adsorption as shown in Figure 2d. The low kinetic energy cutoff gives a reduced work function where initially the bare MoS₂ showed a value close to 4.4 eV. Then it gradually decreases close to about 4.3 eV for the multilayer case. This brings us to a work function difference of about 0.1 eV, which implies that there is weak charge transfer at the interface. The magnitude of the charge transfer in the PTCDI-C4/MoS₂ interface is fairly comparable with the previous investigation of the hydrogen and lead phthalocyanine molecular adsorption on MoS₂.⁵⁶

From the series of surface spectroscopies presented, we propose that the interaction of insulating butyl chains and the contribution of sulfur vacancies at the basal plane of MoS₂ could facilitate an interfacial dipole as we cross from a few layers to a multilayer case schematically shown in Scheme 1a. To summarize the photoelectron spectroscopic results, we propose the schematic energy level alignment at the PTCDI-C4/MoS₂ interface as shown in Scheme 1b. Because the governing force in this noncovalent system is a weak molecule–substrate interaction, no strong overlap hybridization between

Scheme 1. (a) Schematic Illustration of the Proposed Molecular Conformation in Their Respective Cases of Molecular Thicknesses;^a (b) Proposed Scheme of the Energy Level Alignment Diagram at the PTCDI-C4/MoS₂ Interface



^aTop, middle, and below panels are assigned for 5, 3, and 1 min of deposition, respectively.

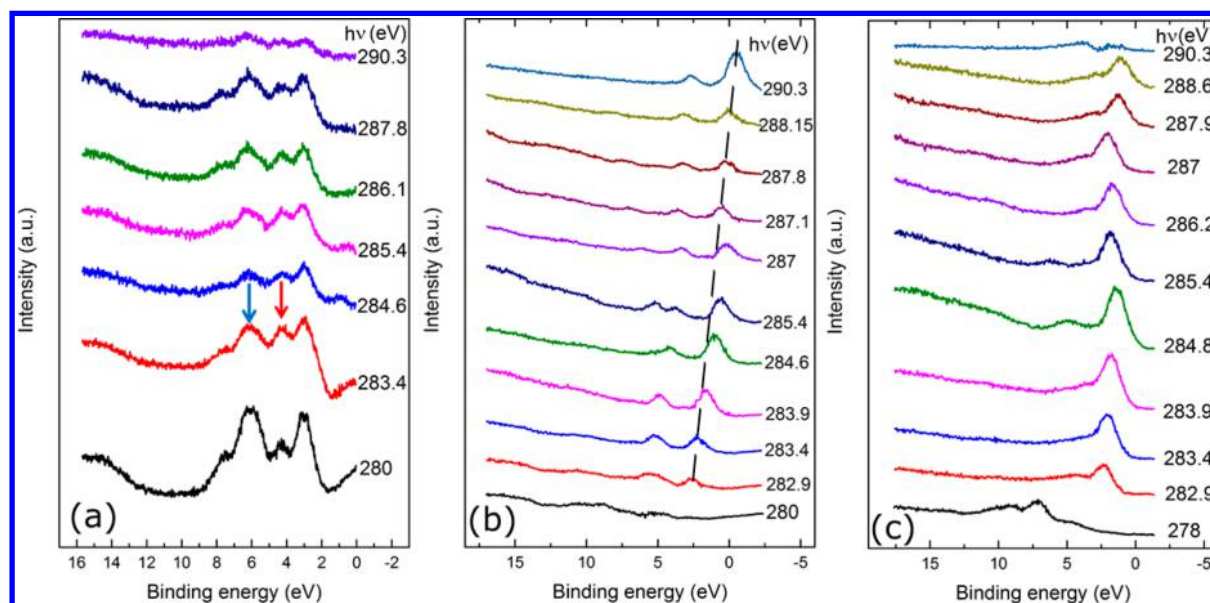


Figure 3. (a) RPES spectra of PTCDI-C4 deposited in 1 min on MoS₂. Red and blue arrows represent the HOMO enhancements. (b) RPES spectra that were taken on 3 min sample. The black dashed line is given as a guide for typical signal originating from C 1s core level excited due to the second-order light contribution. (c) RPES spectra of multilayer thick sample (5 min).

the molecular state and the defect state within MoS₂ layers would be expected to occur.

To examine the previous hypothesis, we have carried out RPES measurements of the aforementioned samples in our synchrotron facility shown in Figure 3. The resonant photoemission spectra for the few layers and multilayer PTCDI-C4 in Figure 3a,b share similar features. Typically, resonant features with the BE value lower (<8 eV) are associated with the resonant enhancement of individual molecular frontier orbitals (HOMO–HOMO-3),²⁷ and their fashions are relatively discrete in energy. On the other hand, featureless resonant structures are usually expected at higher BE (>8 eV), and this event is mostly contributed by the resonant Auger and normal Auger process.

Let us consider the RPES spectrum shown in Figure 3a at the photon energy of 283.4 eV. Here it is shown that a weak HOMO resonant enhancement close to 4 eV (red arrow) and a subsequent peak at 6 eV (blue arrow) indicate a non-negligible photoexcited electron has taken part in the participator decay transition. We note that these features are progressively decayed as a function of the photon energy considering from the off-resonance region (280 eV) across the higher photon energy of 290 eV. Although the HOMO features are somewhat weaker in the case of the 3 min sample (Figure 3b), profound evidence of an extra peak close to the on-resonance regime (285.4 eV) is still observed. It is noteworthy that the second peak is slightly shifted toward higher BE as a function of incident photon energy. This can be attributed to the spectator process in which the emitted photoexcited electron has no constant BE. In other words, we propose that both participator and spectator processes exist during the decay of C 1s core hole in this physisorbed PTCDI-C4/MoS₂ system. For comparison, pronounced HOMO peaks were unambiguously detected in the case of strong chemisorbed PTCDA molecules bound on rutile TiO₂ as previously reported by Cao et al.²⁷ It seems that the physisorption of PTCDI-C4 molecules on MoS₂ led to a weak HOMO contribution in RPES signal. This reaffirmed an intimate interacting atom of the organic molecule and the

underlying substrate is of importance to exhibit strong HOMO resonance enhancement features at the organic/inorganic interfaces.

For comparison, the multilayer sample (5 min) represents a typical scenario because the molecules are usually isolated from the substrate surface. Thus, no significant HOMO enhancement was expected to be observed in the RPES spectra (Figure 3c). According to the previous investigations,²⁵ ultrafast charge-transfer dynamics of multilayer organic films will mainly be governed by the hopping events once the ordered molecular stacks can be realized. On the contrary, our sample here is in a highly disordered regime and, consequently, a weak electronic coupling is expected to be realized because the molecular ordering most likely collapses at the multilayer case. This is in agreement with the proposed Scheme 1a illustration of a highly disordered region responsible for the weak electronic coupling between PTCDI-C4 molecules and MoS₂.

CONCLUSION

We have studied the electronic structure, chemical interaction, and angular dependence of PTCDI-C4 molecules on natural MoS₂ substrates using synchrotron radiation. The carbon absorption edge of NEXAFS measurements at different molecular coverages indicates angular dependence in the case of submonolayer coverage (1 min deposition time). In contrast, the degree of polarization in the other two cases (3 and 5 min deposition times) showed negligible changes in both π^* and σ^* electronic transition as a function of incident photon angle. We propose this is due the highly disordered PTCDI-C4 molecules in the multilayer film. A proposed contribution of weakly interacting alkyl chain at the molecular backbone is manifested in both XPS and UPS results. More importantly, we elucidate the weak electronic coupling between PTCDI-C4 molecules and MoS₂ substrate by the presence of resonant enhancement in the RPES measurement close to the *K*-edge absorption edge. This suggests the nonlocalized molecular state of PTCDI-C4 molecules is weakly coupled to the semiconducting MoS₂ substrate. Thus, our finding provides a better understanding

of PTCDI-C4/MoS₂ interfacial interactions that could be important for the future of 2D van der Waals heterojunction device applications.

■ ASSOCIATED CONTENT

● Supporting Information

The Supporting Information is available free of charge on the ACS Publications website at DOI: 10.1021/acsami.6b14000.

Detailed information on the AFM topographic studies; NEXAFS spectra of 1 min evaporated PTCDI-C4 molecules on HOPG; further analysis on the average tilt angle; XPS deconvolution analysis (PDF)

■ AUTHOR INFORMATION

Corresponding Authors

*(A.) E-mail: phyarr@nus.edu.sg.

*(A.T.S.W.) E-mail: phyweets@nus.edu.sg.

ORCID

Arramel: 0000-0003-4125-6099

Author Contributions

A., A.R., and A.T.S.W. formulated the project. Y.J. Z., S.Z., and A. prepared the sample. A. and X.Y. performed the synchrotron experiments. A. and M.H.H analyzed the experimental data. Q.W. and D.Q. carried out the AFM measurements. J.W. discussed the results. The manuscript was written through contributions of all authors. All authors have given approval to the final version of the manuscript.

Notes

The authors declare no competing financial interest.

■ ACKNOWLEDGMENTS

We acknowledge Wong How Kwong for the XPS measurements of bare MoS₂ substrate. We thank the Center for Advanced 2-Dimensional Materials for the AFM characterization. We appreciate Xiaojiang Yu for his support in the Singapore synchrotron facility and gratefully acknowledge a helpful discussion with Liang Cao. We are also thankful for financial support from the MOE Tier 3 program (MOE2014-T3-1-004). The work at SLS is supported by Singapore National Research Foundation under its Competitive Research Funding (NRF-CRP 8-2011-06), MOE-AcRF Tier-2 (MOE2015-T2-1-099), FRC, and PHC Merlion.

■ REFERENCES

- (1) Ryder, C. R.; Wood, J. D.; Wells, S. A.; Hersam, M. C. Chemically Tailoring Semiconducting Two-Dimensional Transition Metal Dichalcogenides and Black Phosphorus. *ACS Nano* **2016**, *10*, 3900–3917.
- (2) Chuang, S.; Battaglia, C.; Azcatl, A.; McDonnell, S.; Kang, J. S.; Yin, X.; Tosun, M.; Kapadia, R.; Fang, H.; Wallace, R. M.; Javey, A. MoS₂ P-type Transistors and Diodes Enabled by High Work Function MoOx Contacts. *Nano Lett.* **2014**, *14* (3), 1337–1342.
- (3) Mouri, S.; Miyauchi, Y.; Matsuda, K. Tunable Photoluminescence of Monolayer MoS₂ via Chemical Doping. *Nano Lett.* **2013**, *13*, 5944–5948.
- (4) Voiry, D.; Goswami, A.; Kappera, R.; Castro, S. C. d.-C.; Kaplan, D.; Fujita, T.; Chen, M.; Asefa, T.; Chhowalla, M. Covalent Functionalization of Monolayered Transition Metal Dichalcogenides by Phase Engineering. *Nat. Chem.* **2015**, *7*, 45–49.
- (5) Yang, L.; Majumdar, K.; Liu, H.; Du, Y.; Wu, H.; Hatzistergos, M.; Hung, P. Y.; Tieckelmann, R.; Tsai, W.; Hobbs, C.; Ye, P. D. Chloride Molecular Doping Technique on 2D Materials: WS₂ and MoS₂. *Nano Lett.* **2014**, *14*, 6275–6280.
- (6) Sarkar, D.; Xie, X.; Kang, J.; Zhang, H.; Liu, W.; Navarrete, J.; Moskovits, M.; Banerjee, K. Functionalization of Transition Metal Dichalcogenides with Metallic Nanoparticles: Implications for Doping and Gas-Sensing. *Nano Lett.* **2015**, *15*, 2852–2862.
- (7) Nguyen, E. P.; Carey, B. J.; Harrison, C. J.; Atkin, P.; Berean, K. J.; Della Gaspera, E.; Ou, J. Z.; Kaner, R. B.; Kalantar-zadeh, K.; Daeneke, T. Excitation Dependent Bidirectional Electron Transfer in Phthalocyanine-Functionalised MoS₂ Nanosheets. *Nanoscale* **2016**, *8*, 16276–16283.
- (8) Zahn, D. R. T.; Salvan, G.; Paez, B. A.; Scholz, R. Interaction Between Metals and Organic Semiconductors Studied by Raman Spectroscopy. *J. Vac. Sci. Technol., A* **2004**, *22*, 1482–1487.
- (9) Wei, C.; Wang, L.; Huang, C.; Lin, T. T.; Gao, X. Y.; Loh, K. P.; Chen, Z. K.; Wee, A. T. S. Effect of Functional Group (Fluorine) of Aromatic Thiols on Electron Transfer at the Molecule-Metal Interface. *J. Am. Chem. Soc.* **2006**, *128*, 935–939.
- (10) Winget, P.; Schirra, L. K.; Cornil, D.; Li, H.; Coropceanu, V.; Ndione, P. F.; Sigdel, A. K.; Ginley, D. S.; Berry, J. J.; Shim, J.; Kim, H.; Kippelen, B.; Bredas, J. L.; Monti, O. L. Defect-Driven Interfacial Electronic Structures at an Organic/Metal-Oxide Semiconductor Heterojunction. *Adv. Mater.* **2014**, *26*, 4711–4716.
- (11) Racke, D. A.; Kelly, L. L.; Monti, O. L. A. The Importance of Gap States for Energy Level Alignment at Hybrid Interfaces. *J. Electron Spectrosc. Relat. Phenom.* **2015**, *204*, 132–139.
- (12) Zheng, Y. J.; Huang, Y. L.; Chen, Y.; Zhao, W.; Eda, G.; Spataru, C. D.; Zhang, W.; Chang, Y.-H.; Li, L.-J.; Chi, D.; Quek, S. Y.; Wee, A. T. S. Heterointerface Screening Effects between Organic Monolayers and Monolayer Transition Metal Dichalcogenides. *ACS Nano* **2016**, *10*, 2476–2484.
- (13) Peumans, P.; Bulović, V.; Forrest, S. R. Efficient, High-Bandwidth Organic Multilayer Photodetectors. *Appl. Phys. Lett.* **2000**, *76*, 3855–3857.
- (14) Forrest, S. R. Organic–Inorganic Semiconductor Devices and 3,4,9,10-Perylenetetracarboxylic Dianhydride: An Early History of Organic Electronics. *J. Phys.: Condens. Matter* **2003**, *15*, S2599–S2610.
- (15) Tautz, F. S. Structure and Bonding of Large Aromatic Molecules on Noble Metal Surfaces: The Example of PTCDA. *Prog. Surf. Sci.* **2007**, *82*, 479–520.
- (16) Alloway, D. M.; Armstrong, N. R. Organic Heterojunctions of Layered Perylene and Phthalocyanine Dyes: Characterization with UV-Photoelectron Spectroscopy and Luminescence Quenching. *Appl. Phys. A: Mater. Sci. Process.* **2009**, *95*, 209–218.
- (17) Li, C.; Wonneberger, H. Perylene Imides for Organic Photovoltaics: Yesterday, Today, and Tomorrow. *Adv. Mater.* **2012**, *24*, 613–636.
- (18) Ludwig, C.; Gompf, B.; Petersen, J.; Strohmaier, R.; Eisenmenger, W. STM Investigations of PTCDA and PTCDI on Graphite and MoS₂. A Systematic Study of Epitaxy and STM Image Contrast. *Z. Phys. B: Condens. Matter* **1994**, *93*, 365–373.
- (19) Rohlfing, M.; Temirov, R.; Tautz, F. S. Adsorption Structure and Scanning Tunneling Data of a Prototype Organic-Inorganic Interface: PTCDA on Ag(111). *Phys. Rev. B: Condens. Matter Mater. Phys.* **2007**, *76*, 115421-1–115421-16.
- (20) Serkovic Loli, L. N.; Hamoudi, H.; Gayone, J. E.; Martiarena, M. L.; Sánchez, E. A.; Grizzi, O.; Pasquali, L.; Nannarone, S.; Doyle, B. P.; Dablemont, C.; Esaulov, V. A. Growth of N,N'-Bis(1-ethylpropyl)-perylene-3,4,9,10-tetracarboxydiimide Films on Ag (111). *J. Phys. Chem. C* **2009**, *113*, 17866–17875.
- (21) O'Shea, J. N.; Saywell, A.; Magnano, G.; Perdigão, L. M. A.; Satterley, C. J.; Beton, P. H.; Dhanak, V. R. Adsorption of PTCDI on Au(111): Photoemission and Scanning Tunneling Microscopy. *Surf. Sci.* **2009**, *603*, 3094–3098.
- (22) Lament, K.; Kamiński, W.; Mazur, P.; Zuber, S.; Ciszewski, A. Molecular Recognition of PTCDI–C8 Molecules on the Si(110)–(16×2) Surface. *Appl. Surf. Sci.* **2014**, *304*, 50–55.
- (23) Kampen, T. U.; Salvan, G.; Paraiian, A.; Himcinschi, C.; Kobitski, A. Y.; Friedrich, M.; Zahn, D. R. T. Orientation of Perylene Derivatives on Semiconductor Surfaces. *Appl. Surf. Sci.* **2003**, *212*, 501–507.

- (24) Hiroshiba, N.; Hayakawa, R.; Petit, M.; Chikyow, T.; Matsuishi, K.; Wakayama, Y. Structural Analysis and Transistor Properties of Hetero-Molecular Bilayers. *Thin Solid Films* **2009**, *518*, 441–443.
- (25) de Jong, M. P.; Friedlein, R.; Sorensen, S. L.; Öhrwall, G.; Osikowicz, W.; Tengsted, C.; Jönsson, S. K. M.; Fahlman, M.; Salaneck, W. R. Orbital-Specific Dynamic Charge Transfer from Fe(II)-Tetraphenylporphyrin Molecules to Molybdenum Disulfide Substrates. *Phys. Rev. B: Condens. Matter Mater. Phys.* **2005**, *72*, 035448-1–035448-8.
- (26) Cao, L.; Wang, Y.-Z.; Chen, T.-X.; Zhang, W.-H.; Yu, X.-J.; Ibrahim, K.; Wang, J.-O.; Qian, H.-J.; Xu, F.-Q.; Qi, D.-C.; Wee, A. T. S. Charge Transfer Dynamics of 3,4,9,10-Perylene-tetracarboxylic-dianhydride Molecules on Au(111) Probed by Resonant Photoemission Spectroscopy. *J. Chem. Phys.* **2011**, *135*, 174701-1–174701-7.
- (27) Cao, L.; Wang, Y.-Z.; Zhong, J.-Q.; Han, Y.-Y.; Zhang, W.-H.; Yu, X.-J.; Xu, F.-Q.; Qi, D.-C.; Wee, A. T. S. Molecular Orientation and Site Dependent Charge Transfer Dynamics at PTCDA/TiO₂(110) Interface Revealed by Resonant Photoemission Spectroscopy. *J. Phys. Chem. C* **2014**, *118*, 4160–4166.
- (28) Ayzner, A. L.; Nordlund, D.; Kim, D.-H.; Bao, Z.; Toney, M. F. Ultrafast Electron Transfer at Organic Semiconductor Interfaces: Importance of Molecular Orientation. *J. Phys. Chem. Lett.* **2015**, *6*, 6–12.
- (29) Chen, W.; Qi, D. C.; Huang, Y. L.; Huang, H.; Wang, Y. Z.; Chen, S.; Gao, X. Y.; Wee, A. T. S. Molecular Orientation Dependent Energy Level Alignment at Organic–Organic Heterojunction Interfaces. *J. Phys. Chem. C* **2009**, *113*, 12832–12839.
- (30) Splendiani, A.; Sun, L.; Zhang, Y.; Li, T.; Kim, J.; Chim, C.-Y.; Galli, G.; Wang, F. Emerging Photoluminescence in Monolayer MoS₂. *Nano Lett.* **2010**, *10*, 1271–1275.
- (31) Eda, G.; Yamaguchi, H.; Voiry, D.; Fujita, T.; Chen, M.; Chhowalla, M. Photoluminescence from Chemically Exfoliated MoS₂. *Nano Lett.* **2011**, *11*, 5111–5116.
- (32) Chhowalla, M.; Shin, H. S.; Eda, G.; Li, L. J.; Loh, K. P.; Zhang, H. The Chemistry of Two-Dimensional Layered Transition Metal Dichalcogenide Nanosheets. *Nat. Chem.* **2013**, *5*, 263–275.
- (33) Huang, Y. L.; Chen, Y.; Zhang, W.; Quek, S. Y.; Chen, C.-H.; Li, L.-J.; Hsu, W.-T.; Chang, W.-H.; Zheng, Y. J.; Chen, W.; Wee, A. T. S. Bandgap Tunability at Single-Layer Molybdenum Disulfide Grain Boundaries. *Nat. Commun.* **2015**, *6*, 6298.
- (34) Schmidt, H.; Giustiniano, F.; Eda, G. Electronic Transport Properties of Transition Metal Dichalcogenide Field-Effect Devices: Surface and Interface effects. *Chem. Soc. Rev.* **2015**, *44*, 7715–7736.
- (35) Hinnemann, B.; Moses, P. G.; Bonde, J.; Jørgensen, K. P.; Nielsen, J. H.; Horch, S.; Chorkendorff, I.; Nørskov, J. K. Biomimetic Hydrogen Evolution: MoS₂ Nanoparticles as Catalyst for Hydrogen Evolution. *J. Am. Chem. Soc.* **2005**, *127*, 5308–5309.
- (36) Addou, R.; Colombo, L.; Wallace, R. M. Surface Defects on Natural MoS₂. *ACS Appl. Mater. Interfaces* **2015**, *7*, 11921–11929.
- (37) <http://www.hqgraphene.com/> (accessed Aug 7, 2016).
- (38) Xiaojiang, Y.; Oliver, W.; Moser, H. O.; Vidyaraj, S. V.; Gao, X. Y.; Wee, A. T. S.; Nyunt, T.; Qian, H.; Zheng, H. New Soft X-ray Facility SINS for Surface and Nanoscale Science at SSSL. *J. Electron Spectrosc. Relat. Phenom.* **2005**, *144–147*, 1031–1034.
- (39) Stöhr, J. *NEXAFS Spectroscopy*, 1st ed.; Springer-Verlag: Berlin, Germany, 1992.
- (40) Breuer, T.; Klues, M.; Witte, G. Characterization of Orientational Order in π -Conjugated Molecular Thin Films by NEXAFS. *J. Electron Spectrosc. Relat. Phenom.* **2015**, *204*, 102–115.
- (41) Okudaira, K. K.; Setoyama, H.; Yagi, H.; Mase, K.; Kera, S.; Kahn, A.; Ueno, N. Study of Excited States of Fluorinated Copper Phthalocyanine by Inner Shell Excitation. *J. Electron Spectrosc. Relat. Phenom.* **2004**, *137–140*, 137–140.
- (42) Lanzilotto, V.; Lovat, G.; Otero, G.; Sanchez, L.; López, M. F.; Méndez, J.; Martín-Gago, J. A.; Bavdek, G.; Floreano, L. Commensurate Growth of Densely Packed PTCDI Islands on the Rutile TiO₂(110) Surface. *J. Phys. Chem. C* **2013**, *117*, 12639–12647.
- (43) Fratesi, G.; Lanzilotto, V.; Stranges, S.; Alagia, M.; Brivio, G. P.; Floreano, L. High Resolution NEXAFS of Perylene and PTCDI: A Surface Science Approach to Molecular Orbital Analysis. *Phys. Chem. Chem. Phys.* **2014**, *16*, 14834–14844.
- (44) Wei, C.; Qi, D.-C.; Wee, A. T. S. NEXAFS Studies of Molecular Orientations at Molecule–Substrate Interfaces. In *The Molecule–Metal Interface*; Koch, N. U., Wee, A. T. S., Eds.; Wiley-VCH: Weinheim, Germany, 2013; Chapter 5, pp 119–151.
- (45) Cao, L.; Wang, Y.; Zhong, J.; Han, Y.; Zhang, W.; Yu, X.; Xu, F.; Qi, D.-C.; Wee, A. T. S. Electronic Structure, Chemical Interactions and Molecular Orientations of 3,4,9,10-Perylene-tetracarboxylic-dianhydride on TiO₂(110). *J. Phys. Chem. C* **2011**, *115*, 24880–24887.
- (46) Schlettwein, D.; Back, A.; Schilling, B.; Fritz, T.; Armstrong, N. R. Ultrathin Films of Perylenedianhydride and Perylenebis-(dicarboximide) Dyes on (001) Alkali Halide Surfaces. *Chem. Mater.* **1998**, *10*, 601–612.
- (47) Chesterfield, R. J.; McKeen, J. C.; Newman, C. R.; Frisbie, C. D.; Ewbank, P. C.; Mann, K. R.; Miller, L. L. Variable Temperature Film and Contact Resistance Measurements on Operating n-Channel Organic Thin Film Transistors. *J. Appl. Phys.* **2004**, *95*, 6396–6405.
- (48) Malenfant, P. R. L.; Dimitrakopoulos, C. D.; Gelorme, J. D.; Kosbar, L. L.; Graham, T. O.; Curioni, A.; Andreoni, W. N-type Organic Thin-Film Transistor with High Field-Effect Mobility Based on a N,N'-dialkyl-3,4,9,10-Perylene-tetracarboxylic-diimide Derivative. *Appl. Phys. Lett.* **2002**, *80*, 2517–2519.
- (49) Rolin, C.; Vasseur, K.; Schols, S.; Jouk, M.; Duhoux, G.; Müller, R.; Genoe, J.; Heremans, P. High Mobility Electron-Conducting Thin-Film Transistors by Organic Vapor Phase Deposition. *Appl. Phys. Lett.* **2008**, *93*, 033305-1–033305-3.
- (50) Cho, S. W.; Newby, D.; DeMasi, A.; Smith, K. E.; Piper, L. F. J.; Jones, T. S. Determination of the Individual Atomic Site Contribution to the Electronic Structure of 3,4,9,10-Perylene-tetracarboxylic-dianhydride (PTCDA). *J. Chem. Phys.* **2013**, *139*, 184711-1–184711-7.
- (51) Cao, L.; Zhang, W.; Han, Y.; Chen, T.; Zheng, Z.; Wan, L.; Xu, F.; Ibrahim, K.; Qian, H.; Wang, J. Angular Dependent NEXAFS Study of the Molecular Orientation of PTCDA Multilayers on Au (111) Surface. *Chin. Sci. Bull.* **2011**, *56*, 3575–3577.
- (52) McDonnell, S.; Addou, R.; Buie, C.; Wallace, R. M.; Hinkle, C. L. Defect-Dominated Doping and Contact Resistance in MoS₂. *ACS Nano* **2014**, *8*, 2880–2888.
- (53) Addou, R.; McDonnell, S.; Barrera, D.; Guo, Z.; Azcatl, A.; Wang, J.; Zhu, H.; Hinkle, C. L.; Quevedo-Lopez, M.; Alshareef, H. N.; Colombo, L.; Hsu, J. W. P.; Wallace, R. M. Impurities and Electronic Property Variations of Natural MoS₂ Crystal Surfaces. *ACS Nano* **2015**, *9*, 9124–9133.
- (54) Smyth, C. M.; Addou, R.; McDonnell, S.; Hinkle, C. L.; Wallace, R. M. Contact Metal–MoS₂ Interfacial Reactions and Potential Implications on MoS₂-Based Device Performance. *J. Phys. Chem. C* **2016**, *120*, 14719–14729.
- (55) Komsa, H.-P.; Krashenninnikov, A. V. Native Defects in Bulk and Monolayer MoS₂ from First Principles. *Phys. Rev. B: Condens. Matter Mater. Phys.* **2015**, *91*, 125304-1–125304-17.
- (56) Nobuo, U.; Katsumi, S.; Masahiro, M.; Masato, K.; Kazuyuki, S. Growth of Pb-Phthalocyanine Thin Films on MoS₂ Surfaces Studied by Means of Low-Energy Electron Transmission Spectroscopy. *Jpn. J. Appl. Phys.* **1994**, *33*, 319–323.